Zaynobidinov Sirojiddin Zaynobidinovich
Andijon davlat universiteti f-m.f.d. akademik
Boboyev Akromjon Yo‘ldashboevich
Andijon davlat universiteti f-m.f.d.
aboboevscp@gmail.com
Yo‘lchiyev Shaxriyor Xusanovich
Andijon pedagogika instituti f-m.f.d.proffessor
Soliyev Iqboljon Maxammadjonovich
Andijon davlat universiteti mustaqil tadqiqotchisi
Iqboljonsoliev45@gmail.com

UDK: 621.315.592.3:538.91

GAAS TAGLIGIGA O‘STIRILGAN $(ZnSe)_{1-x-y}(Ge_2)_x(GaAs_{1-\delta}Bi_\delta)_y$ EPITAKSIAL QATLAMLARDA Ge NANOKRISTALLAR HAMDA $GaAs_{1-\delta}Bi_\delta$ KVANT QUDUQLARINING SHAKLLANISHI

Annotatsiya: Ushbu tadqiqotda Bi tarkibli eritmadan suyuq fazali epitaksiya usuli yordamida (100) yo‘nalishli n-GaAs substratlarida o‘stirilgan $(ZnSe)_{1-x-y}(Ge_2)_x(GaAs_1-\delta Bi\delta)_y$ epitaksial qatlamlarning tuzilma va elektrofizik xossalari o‘rganildi. Rentgen mikroanalizi natijasida qatlam qalinligi bo‘ylab ZnSe, Ge_2 va $GaAs_1-\delta Bi\delta$ komponentlarining kontsentratsiyasi bosqichma-bosqich o‘zgarib borishi aniqlanib, ularning maksimal molyar ulushlari x = 0,725 va y = 0,638 qiymatlarida kuzatildi. Rentgen difraksiyasi tahlili natijalariga ko‘ra, hosil bo‘lgan qatlam sferolit tuzilishga ega bo‘lib, (100) yo‘nalishida o‘sganligi tasdiqlandi. Panjara mos kelmasligi (4,8%) Ge nanokristallar (~47 nm) hamda $GaAs_1-\delta Bi\delta$ kvant quduqlar (~43 nm) hosil bo‘lishiga olib keldi. $GaAs_1-\delta Bi\delta$ materialining tarmoqli oralig‘i (1,21 eV) asosiy qatlamning qiymatidan (1,53 eV) kichikligi kvant quduqlar shakllanganini tasdiqlaydi. Olingan natijalar optoelektronika uchun mo‘ljallangan yarimo‘tkazuvchi qattiq eritmalarda nanostrukturalarning o‘z-o‘zidan tashkil topish jarayonini chuqurroq tushunishga yordam beradi.

Kalit so‘zlar: $(ZnSe)_{1-x-\gamma}(Ge_2)_x(GaAs_1-\delta Bi\delta)_\gamma$ qattiq eritma, epitaksial qatlamlar, GaAs substrati, suyuq fazali epitaksiya, rentgen difraksiyasi, rentgen mikroanalizi, Ge nanokristallar, $GaAs_1-\delta Bi\delta$ kvant quduqlari, panjara mos kelmasligi, nanoobyektlar, sferolit tuzilma, kristallografik yo‘nalish, tarmoqli oralig‘ini boshqarish, nuqsonlar keltirib chiqargan deformatsiya, optoelektron materiallar

Зайнабиддинов Сирожиддин Зайнабиддинович
Доктор физико-математических наук, академик,
Андижанский государственный университет

Бобаев Акромжон Йулдашбоевич
Доктор физико-математических наук,
Андижанский государственный университет
E-mail: **aboboevscp@gmail.com**
Юлчиев Шахрияр Хусанович
Доктор физико-математических наук, профессор,
Андижанский педагогический институт
Солиев Икболжон Махаммаджонович
Независимый исследователь,
Андижанский государственный университет
E-mail: **iqboljonsoliev45@gmail.com**

ОБРАЗОВАНИЕ НАНОКРИСТАЛЛОВ GE И КВАНТОВЫХ ЯМ $GaAs_{1-\delta}Bi_{\delta}$ В ЭПИТАКСИАЛЬНЫХ СЛОЯХ $(ZnSe)_{1-x-y}(Ge_2)_x(GaAs_{1-\delta}Bi_{\delta})_y$ НА GaAs

Аннотация: В данном исследовании изучены структурные и электрофизические свойства эпитаксиальных слоёв $(ZnSe)_{1-x-\gamma}(Ge_2)_x(GaAs_1-\delta Bi\delta)_\gamma$, выращенных на подложках (100) n-GaAs методом жидкофазной эпитаксии из расплава, содержащего висмут. Рентгеновский микроанализ выявил постепенные изменения концентраций ZnSe, Ge_2 и $GaAs_1-\delta Bi\delta$ по толщине плёнки, при этом максимальные мольные доли составляли x = 0,725 и y = 0,638. Рентгеноструктурный анализ подтвердил наличие структуры сфалерита с ориентацией (100). Несоответствие постоянных решёток (4,8%) привело к образованию нанокристаллов Ge (~47 нм) и квантовых ям $GaAs_1-\delta Bi\delta$ (~43 нм). Ширина запрещённой зоны $GaAs_1-\delta Bi\delta$ (1,21 эВ) оказалась меньше, чем у основного слоя (1,53 эВ), что подтверждает формирование квантовых ям. Полученные результаты способствуют более глубокому пониманию процессов самоорганизации наноструктур в полупроводниковых твёрдых растворах для оптоэлектронных применений.

Ключевые слова: твёрдый раствор $(ZnSe)_{1-x-\gamma}(Ge_2)_x(GaAs_1-\delta Bi\delta)_\gamma$, эпитаксиальные слои, подложка GaAs, жидкофазная эпитаксия, рентгеноструктурный анализ, рентгеновский микроанализ, нанокристаллы Ge, квантовые ямы $GaAs_1-\delta Bi\delta$, несовпадение параметров решётки, нанообъекты, структура сфалерита, кристаллографическая ориентация, инженерия запрещённой зоны, деформации, вызванные дефектами, оптоэлектронные материалы.

Zaynobidinov Sirojiddin Zaynobidinovich
Doctor of Physical and Mathematical Sciences, Academician,
Andijan State University
Boboyev Akromjon Yo‘ldashboevich
Doctor of Physical and Mathematical Sciences,
Andijan State University
E-mail: **aboboevscp@gmail.com**
Yo‘lchiyev Shakhriyor Khusanovich
Doctor of Physical and Mathematical Sciences, Professor,
Andijan Pedagogical Institute
Soliyev Iqboljon Makhammadjonovich
Independent Researcher,
Andijan State University
E-mail: **iqboljonsoliev45@gmail.com**

FORMATION OF GE NANOCRYSTALS AND $GaAs_{1-\delta}Bi_{\delta}$ QUANTUM WELLS IN $(ZnSe)_{1-x-y}(Ge_2)_x(GaAs_{1-\delta}Bi_{\delta})_y$ EPITAXIAL LAYERS ON GaAs

Annotation: This study investigates the structural and electrophysical properties of $(ZnSe)_{1-x-y}(Ge_2)_x(GaAs_{1-\delta}Bi_{\delta})_y$ epitaxial layers grown on (100) n-GaAs substrates using liquid-phase epitaxy from a Bi-containing melt. X-ray microanalysis revealed gradual variations in ZnSe, Ge_2, and $GaAs_1$–δBiδ concentrations across the film thickness, with maximum molar fractions at x = 0.725 and y = 0.638. X-ray diffraction confirmed a sphalerite structure with (100) orientation. Lattice mismatch (4.8%) led to the formation of Ge nanocrystals (~47 nm) and $GaAs_{1-\delta}Bi_{\delta}$ quantum wells (~43 nm). The $GaAs_{1-\delta}Bi_{\delta}$ band gap (1.21 eV) is lower than that of the main layer (1.53 eV), confirming quantum well formation. These results provide insights into nanostructure self-organization in semiconductor solid solutions for optoelectronic applications.

Keywords: $(ZnSe)_{1-x-y}(Ge_2)_x(GaAs_{1-\delta}Bi_{\delta})_y$ solid solution, epitaxial layers, GaAs substrate, liquid-phase epitaxy, X-ray diffraction, X-ray microanalysis, Ge nanocrystals, $GaAs_1$–δBiδ quantum wells, lattice mismatch, nano-objects, sphalerite structure, crystallographic orientation, band gap engineering, defect-induced strain, optoelectronic materials.

Introduction. Solving a number of scientific and technical problems associated with expanding the functionality of semiconductor electronic products and nano- and microelectronic systems over a wide temperature range is one of the urgent issues of modern materials science [1; pp. 78–83; 2; pp. 60–66]. Despite the availability of a considerable number of publications devoted to this problem, the degree of study of the peculiarities of impurity atom doping of Si, Ge, GaAs, and

other semiconductor single crystals—which create various energy levels within the band gap—as well as the behavior of defects introduced during growth or by neutron irradiation, and their influence on current transport in both semiconductor materials and multilayer structures, remains insufficiently explored.

At the same time, determining the optimal technological conditions for the formation of alloyed and defect-free epitaxial thin films, as well as selecting the necessary components and impurity atoms that enable targeted control of their properties, is of great scientific and practical interest. The results of molecular-level studies of impurities, the behavior of nanocrystallites in solid solutions, and the dependence of current transport processes on the basic material composition, particularly the interaction between nanocrystallites in semiconductor materials, remain inadequately understood.

In this regard, this section of the monograph presents experimental results of the X-ray structural characterization of $(ZnSe)_{1-x-y}(Ge_2)_x(GaAs_{1-\delta}Bi_\delta)_y$ solid solutions grown on (100)-oriented n-GaAs substrates from a Bi-containing melt using the liquid-phase epitaxy method under forced-cooling conditions.

Experimental procedure. To grow $(ZnSe)_{1-x-y}(Ge_2)_x(GaAs_{1-\delta}Bi_\delta)_y$ epitaxial films on GaAs substrates, we used the liquid-phase epitaxy (LPE) method from a limited volume of a solution–melt. The investigated films were grown in the crystallization temperature range of 750–650 °C at a substrate cooling rate of 1 °C/min**.** The obtained $(ZnSe)_{1-x-y}(Ge_2)_x(GaAs_{1-\delta}Bi_\delta)_y$ epitaxial films exhibited p-type conductivity, with a charge carrier mobility of 357 $cm^2/(V\cdot s)$ and a carrier concentration of $p = 5 \times 10^{17}$ cm^{-3}**.**The chemical composition of the obtained $(ZnSe)_{1-x-y}(Ge_2)_x(GaAs_{1-\delta}Bi_\delta)_y$ epitaxial layers was studied using a JEOL JSM-5910LV X-ray microanalyzer. Based on the results of X-ray microanalysis, the distribution profiles of ZnSe, Ge_2, and $GaAs_{1-\delta}Bi_\delta$ compounds across the thickness of the epitaxial layer were determined (Fig.1).

Experimental results and discussion. From the figure, it can be seen that with increasing thickness of the $(ZnSe)_{1-x-y}(Ge_2)_x(GaAs_{1-\delta}Bi_\delta)_y$ epitaxial layer, the molar fractions of Ge_2 and $GaAs_{1-\delta}Bi_\delta$ gradually increase, reaching their maximum values at x = 0.725 and y = 0.638, respectively. This indicates a high degree of supersaturation of the Bi-containing melt with Ge_2 and $GaAs_{1-\delta}Bi_\delta$ components in the crystallization zone. Subsequently, the molar contents of Ge_2 and $GaAs_{1-\delta}Bi_\delta$ decrease gradually, reaching x = 0.23 and y = 0.3 near the surface of the epitaxial layer. Since the epitaxial layer growth occurs within a limited melt volume, and the solubility of $GaAs_{1-\delta}Bi_\delta$ and Ge in liquid bismuth is approximately three and two times lower, respectively, than that of ZnSe, this leads to a gradual reduction in their molar contents along the growth direction. Distribution profile of ZnSe,

Ge_2, and $GaAs_{1-\delta}Bi_\delta$ compound molecules along the thickness of the $(ZnSe)_{1-x-y}(Ge_2)_x(GaAs_{1-\delta}Bi_\delta)_y$ epitaxial layer.

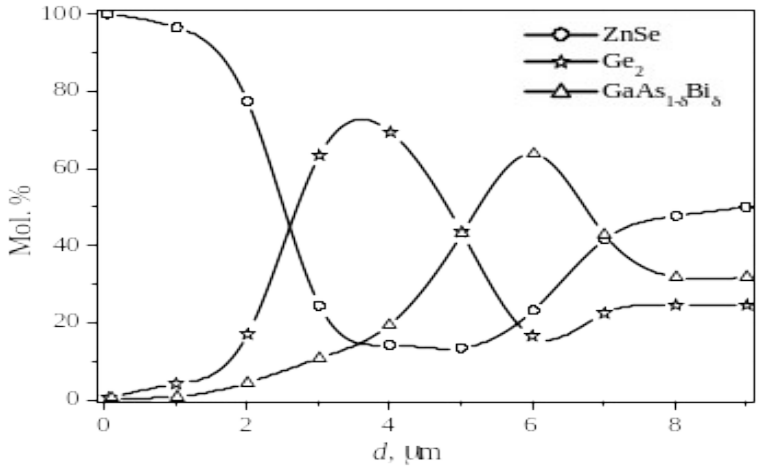

Figure 1.Distribution profile of ZnSe, Ge_2, and $GaAs_{1-\delta}Bi_\delta$ compound molecules along the thickness of the $(ZnSe)_{1-x-y}(Ge_2)_x(GaAs_{1-\delta}Bi_\delta)_y$ epitaxial layer.

Starting from a surface depth of about 1 μm, the molar concentrations of Ge and $GaAs_1$−δBiδ do not exceed 23% and 30%, respectively. Thus, it was found that the grown epitaxial films represent a substitutional solid solution of $(ZnSe)_{1-x-y}(Ge_2)_x(GaAs_{1-\delta}Bi_\delta)_y$, in which the molar fractions of the constituent components gradually vary within the ranges $0 \le x \le 0.725$ and $0 \le y \le 0.638$. It was revealed that, between the substrate and the surface region of the film, a layer enriched with Ge and $GaAs_{1-\delta}Bi_\delta$ compounds having a narrower energy band gap is formed.

The structural and phase states of *n*-GaAs-*p*-$(GaAs)_{1-x-y}(Ge_2)_x(ZnSe)_y$ heterostructures were investigated using an Empyrean Malvern third-generation X-ray diffractometer. The X-ray diffraction measurements were carried out in Bragg–Brentano geometry within the 2θB range of 15° to 100°, at a constant scanning rate of 1°/min. The OriginPro 2019 software was used to determine the highest observed structural peaks. Figure 2 presents the X-ray diffraction pattern of the GaAs substrate, where a series of selective structural reflections of the {H00} type (where N = 1, 2, 3, …) characteristic of the (100) crystallographic orientation are observed.

At the diffraction angles of 2θ = 58.8° and 2θ = 66.25°, the β and α components of the main structural (400)GaAs reflection were observed. A noticeable splitting of the main structural line into its α_1 and α_2 radiation components, while maintaining the intensity ratio of $I(\alpha_1) = 2 \cdot I(\alpha_2)$, indicates the presence of slight elastic microstrains in the crystal lattice near the surface regions of the GaAs substrate.

Based on the experimental values of the main structural (400) reflection, the lattice constant was determined to be 0.5653 nm, which is slightly higher than the tabulated value for gallium arsenide a_{GaAs} = 0.5646 [4; pp.138]. Here, θ denotes the diffraction angle (half of the Bragg angle, 2θ(B)). Additional confirmation of this result is provided by the presence of a weak structural reflection in the (500) direction at d/n = 0.1128 nm (2θ = 86.1°)**,** which is normally forbidden for sphalerite structures. According to the extinction law, such a line should be absent in the X-ray diffraction pattern of a perfect sphalerite GaAs lattice. The appearance of this reflection indicates the presence of micro-defects or local distortions in the GaAs crystal lattice [5; pp. 55–57]. The relative intensity ratio of the (500) to (400) reflections was found to be I(500)/I(400) = 2.74×10⁻⁴**,** which is slightly greater than 10⁻⁴, confirming the existence of minor microstrains in the lattice [6; pp. 77–81].

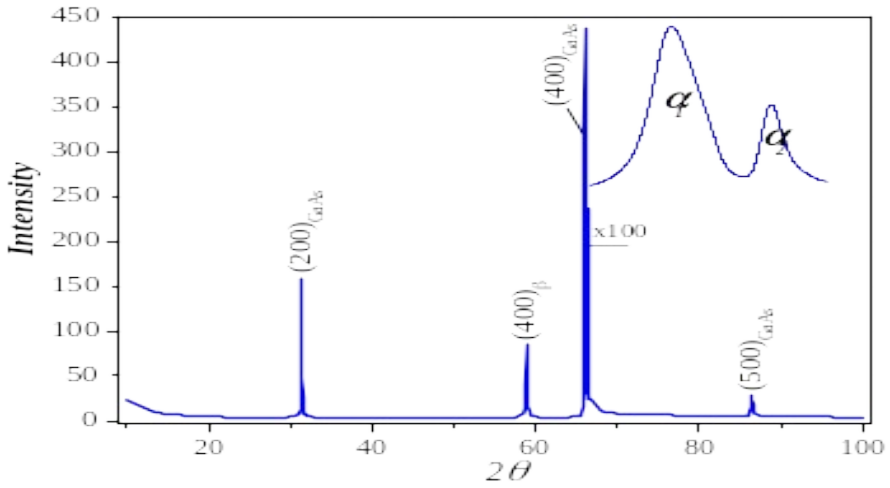

Figure 2. X-ray diffraction pattern of the GaAs substrate.

Such regions of lattice distortion lead to an increase in the lattice constant of the substrate crystal. This value was determined using the extrapolation function proposed by Nelson–Riley [3; pp. 56–59].

$$f = (1/2) \cdot [(\mathrm{Cos}^2\theta/\theta + (\mathrm{Cos}^2\theta/\mathrm{Sin}\theta)], \quad (1)$$

Furthermore, the narrow half-width (FWHM = 0.008 rad) and high intensity (4.5×10⁴ imp·s⁻¹) of the main (400) GaAs reflection, together with the monotonic nature of the inelastic background**,** demonstrate the high structural perfection of the GaAs single-crystal substrate. The X-ray diffraction pattern of the $(ZnSe)_{1-x-y}(Ge_2)_x(GaAs_{1-\delta}Bi_\delta)_y$ epitaxial layer is shown in Figure 3.4.3**,** indicating that the grown film surface belongs to the (100) crystallographic orientation. From the diffraction data, it is observed that the intensity of the (400) reflection decreased by 11% and shifted toward smaller scattering angles (see Fig. 3**)**. The intensity of the

(200) reflection decreased 2.8 times compared to that of the substrate diffraction pattern. These observed changes reflect the modification of the crystal lattice of the solid solution $(ZnSe)_{1-x-\gamma}(Ge_2)_x(GaAs_1-\delta Bi\delta)_\gamma$. Based on the (200) and (400) reflections and using expression (1), the lattice parameter of the epitaxial films was determined to be 0.5663 nm**.** This value is greater than that of the GaAs substrate and very close to the tabulated value for zinc selenide **(**$a_{(ZnSe)}$ = 0.566 nm**).** This indicates that the crystal lattice of the $(ZnSe)_{1-x-y}(Ge_2)_x(GaAs_{1-\delta}Bi_\delta)_y$ solid solution tends to approach that of the ZnSe semiconductor, meaning that the ZnSe compound forms the dominant base structure of the epitaxial layer. Therefore, at the scattering angles 2θ = 56.1° and 2θ = 89.6°, weak structural reflections with crystallographic orientations of (222) ZnSe at d/n = 0.1636 nm and (333) ZnSe at d/n = 0.2831 nm, respectively, were observed. According to the extinction rules for sphalerite-type structures based on ZnSe with a (100) crystallographic orientation, the appearance of reflections of the (222) and (333) types [7; p. 597] indicates the formation of microdefects in the crystal lattice of the layers.

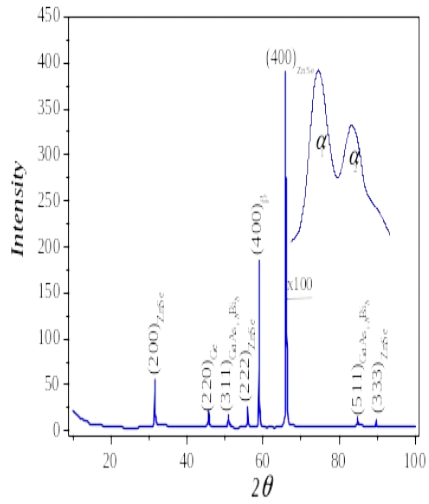

Figure 3. X-ray diffraction pattern of the $(ZnSe)_{1-x-y}(Ge_2)_x(GaAs_{1-\delta}Bi_\delta)_y$ epitaxial layer

As additional confirmation, it was found that in the X-ray diffraction pattern of the $(ZnSe)_{1-x-y}(Ge_2)_x(GaAs_{1-\delta}Bi_\delta)_y$ solid solution, the level of the inelastic background in the small and medium scattering angle ranges (10°–60°) is about 9% higher than that of the substrate diffraction pattern. This fact suggests the accumulation of elastic strain energy within the film lattice, leading to the formation of microstresses. The presence of such microdistortions in the crystal lattice may cause the formation of various nano-objects. The appearance of a structural reflection at the scattering angle 2θ = 45.3° with d/n = 0.1001 nm

corresponding to the (220) orientation confirms the formation of nano-objects in the crystal lattice, and this diffraction line is attributed to Ge nanocrystallites**.** Using the following expression, the sizes of the blocks (subcrystallites) forming the film and the sizes of the Ge nanocrystals were determined from the full width at half maximum (FWHM) of the (400) and (220) structural reflections [8; pp. 15–17]:

$$D = K\lambda / (\beta \cos\Theta), \quad (2)$$

where D is the crystallite size, **λ** is the X-ray wavelength (in our case, 0.154 nm**),** θ is the scattering angle (half of the diffraction angle 2θ(B)**),** β is the physical broadening of the diffraction line (the full width at half maximum, FWHM), and K ≈ 0.94 is the shape factor coefficient [9; pp. 15–17].

$$\beta = \frac{1}{2}\left(B - b + \sqrt{B(B-b)}\right) \quad (3)$$

Here, B is the apparent broadening of the diffraction peak, and b is the apparent geometric broadening. Calculations of D values using the above formula showed that the size of the subcrystallites in the solid solution is about 60 nm, while the size of the Ge nanocrystallites is approximately 47 nm. The lattice parameter of Ge nanocrystals was experimentally determined using Equation (1), and it was found to be a(Ge) = 0.5659 nm, which is very close to its tabulated value of a(Ge) = 0.5657 nm. Thus, in the defect-prone regions of the film matrix lattice, paired Ge atoms partially substitute ZnSe molecules, while the remaining atoms participate in the formation of Ge nanocrystals with an average size of 47 nm at the subcrystallite boundaries of the film. Additionally, two weak structural reflections were observed at diffraction angles of 2θ = 50.9° and 2θ = 84.8°, corresponding to d/n = 0.1791 nm for the (311) plane and d/n = 0.1143 nm for the (511) plane. The analysis confirmed that these reflections belong to the $GaAs_{1-\delta}Bi_{\delta}$ compound. Based on the experimental results of these (311) and (511) reflections and using Equation (1), the lattice constant of the $GaAs_{1-\delta}Bi_{\delta}$ phase was determined to be 0.5941 nm.
The lattice mismatch between the base crystal lattice of the layer and the $GaAs_{1-\delta}Bi_{\delta}$ compound was calculated using the following expression [10; pp. 112–115].

$$\xi = 2|a_{m.s} - a_{GaAsBi}| / (a_{m.s} + a_{GaAsBi}), \quad (4)$$

In our case, this value equals 0.048, that is, the lattice mismatch of the (100) GaAsBi/ZnSe system amounts to 4.8%**.** Such a difference, in turn, leads to the formation of nano-objects in the near-surface regions of the film. Moreover, according to the authors of [49; pp. 33–37], based on the covalent bond energies of the atoms of the nanoinclusions and the base layer materials, these nano-objects

can be classified as “quantum dots” or “quantum wells” as follows: when the band gap of the nanoinclusion ($E_{g,A}$) is greater than that of the main semiconductor layer ($E_{g,B}$) , i.e., ($E_{g,A} > E_{g,B}$), quantum dots are formed; on the contrary, when ($E_{g,A} < E_{g,B}$), quantum wells are formed. In addition, the band gap energy of the $GaAs_{1-\delta}Bi_{\delta}$ compound — one of the components of the solid solution — was calculated using the following expression [11; pp. 33–37]:

$$E_{GaAsBi} = (1-\delta)E_{g,GaAs} + (\delta)E_{g,GaBi} - \xi(\delta)(1-\delta) \quad (5)$$

Here, δ represents the relative content of As and Bi atoms in the $GaAs_{1-\delta}Bi_{\delta}$ compound, determined from X-ray spectral microanalysis results, and its value is δ = 0.125**.** The parameter **ξ** corresponds to the lattice mismatch between GaAs and GaBi compounds, determined using expression (4)**,** and in our case it equals 0.18**.** Based on the calculations, the band gap energy of the $GaAs_{1-\delta}Bi_{\delta}$ compound was found to be 1.21 eV, which is smaller than the experimentally determined value of the main epitaxial layer band gap ($E_{m.s}$ = 1.53 eV). This, in turn, indicates that $GaAs_{1-\delta}Bi_{\delta}$ inclusions spontaneously form quantum wells in the near-surface regions of the film. The size of these quantum wells, calculated using the experimental values of the (311) and (511) diffraction reflections and expression (3.4.2)**,** was found to be 43 nm**.**

Conclusion. In this study, the structural and electrophysical properties of $(ZnSe)_{1-x-\gamma}(Ge_2)_x(GaAs_1-\delta Bi\delta)_{\gamma}$ epitaxial films grown on (100)-oriented GaAs substrates using the liquid-phase epitaxy (LPE) method were experimentally investigated. The films were found to have a sphalerite crystal structure and a (100) crystallographic orientation. X-ray microanalysis revealed a gradual variation in the molar fractions of Ge_2 and $GaAs_1-\delta Bi\delta$ across the thickness of the epitaxial layers, with maximum values of x = 0.725 and y = 0.638 in the crystallization zone, decreasing toward the surface. This indicates a substitutional solid solution with a high degree of compositional control. A layer enriched with Ge and $GaAs_1-\delta Bi\delta$ compounds, characterized by a narrower energy band gap, formed between the substrate and the near-surface regions of the film. X-ray diffraction studies showed slight elastic microstrains in the GaAs substrate near the surface, while the epitaxial layers exhibited lattice parameters close to those of ZnSe, indicating that ZnSe forms the dominant base structure. The analysis also revealed the formation of Ge nanocrystallites with an average size of 47 nm at the boundaries of subcrystallites, where paired Ge atoms partially substitute ZnSe molecules.

Furthermore, $GaAs_1-\delta Bi\delta$ inclusions spontaneously formed quantum wells in the near-surface regions of the films, with a size of approximately 43 nm, as determined from (311) and (511) diffraction reflections. The lattice mismatch

between GaAs and $GaAs_1$–δBiδ was calculated to be 4.8%, which contributes to the formation of nano-objects in the near-surface layers.

Overall, the results demonstrate that $(ZnSe)_{1-x-\gamma}(Ge_2)_x(GaAs_1-\delta Bi\delta)_\gamma$ epitaxial films possess high structural perfection, controllable compositional gradients, and the capability to form nanostructures such as Ge nanocrystals and quantum wells, making them promising materials for applications in optoelectronic and nanoelectronic devices.

Thus, it was established that the grown epitaxial films represent substitutional solid solutions of the type $(ZnSe)_{1-x-y}(Ge_2)_x(GaAs_{1-\delta}Bi_\delta)_y$, in which the molar contents of the components gradually vary within the ranges $0 \le x \le 0.725$ and $0 \le y \le 0.638$**.** Between the substrate and the near-surface regions of the film, a layer enriched with Ge and $GaAs_{1-\delta}Bi_\delta$ components—characterized by a narrow band gap—was formed. The grown solid solutions possess a sphalerite structure and belong to the (100) crystallographic orientation of single crystals.

In defect-prone regions of the film matrix lattice, paired Ge atoms partially substitute ZnSe molecules**,** while the remaining Ge atoms participate in the formation of Ge nanocrystals with an average size of 47 nm at the subcrystalline grain boundaries. The $GaAs_1$–δBiδ inclusions, in turn, spontaneously form quantum wells in the near-surface regions of the film, the size of which—determined from the experimental data of the (311) and (511) structural reflections using expression (2)—was found to be 43 nm.

References:

1. Белоус А.И Ефименко С.А. Турцевич А.С. Полупроводниковая силовая электроника. Москва: Техносфера, 2013. 216 с.

2. Марков В.Ф., Мухамедзянов Х.Н., Маскаева Л.Н. Материалы современной электроники. Екатеринбург Издательство Уральского университета, 2014. 272 с.

3. Сетюков О.А., Самойлов А.И. Влияние юстировки рентгеновского дифрактометра на зависимость периода решетки от экстраполяционной функции Нельсона–Райли. // **Научные публикatsii сотрудников ВИАМ.** 2011. Том.77 Вып. 8. С.

4. Равделя А., Пономаревой А.М. Краткий справочник физико–химических величин. Ленинград: Химия, 1983. 138 с.

5. Зайнабидинов С.З., СаидовА.С., Бобоев А.Й., Усмонов Ж.Н. Особенности свойств поверхности полупроводникового твердого раствора$(GaAs)_{1-x-y}(Ge_2)_x(ZnSe)_y$ с квантовыми точками ZnSe. // Поверхность. Рентгеновские, синхротронные и нейтронные исследования. 2021. № 1. С. 107.

6. Шулпина И.Л., Кютт Р.Н., Ратников В.В., Прохоров И.А., Безбах И.Ж., Щеглов М.П. Методы рентгеновской дифракционной диагностики сильнолегированных монокристаллов полупроводников. // Журнал технической физики. -2010. -Том 80(4). -С.105.

7. Ширяев А.А., Золотов Д.А., Супрун Е.М., Дьячкова И.Г., Ивахненко С.А., Асадчиков В.Е. Вклад структурных дефектов в интенсивность квазизапрещенных рентгеновских отражений алмаза: сравнение данных рентгеновской топографии и инфракрасной спектроскопии. // Письма в Журнал экспериментальной и теоретической физики. 2020. Том 111. Вып. 9. С. 597.

8. Иванов А.Н., Расторгуев Л.Н., Скаков Ю.А., Уманский Я.С. Кристаллография, рентгенография и электронная микроскопия. Москва: Металлургия, 1982. 632 с.

9. Комков О.С. Расчёт полупроводниковых гетеропереходов. Учеб.-метод. пособие. СПб.: Изд-во СПбГЭТУ «ЛЭТИ», 2018. 52 с.

10. Saidov A.S., Saidov M.S., Usmonov Sh.N., Leiderman, A.Yu. Kalanov M.U., Gaimnazarov K.G., Kurmantaev A.N. Growth of $(GaAs)_{1-x}(ZnSe)_x$ solid solution films and investigation of their structural and some photoelectric properties. // Physics of the Solid State. 2011, Vol. 53. No. 10. P. 2012.

11. Комков О.С. Расчёт полупроводниковых гетеропереходов. Учеб.-метод. пособие. СПб.: Изд-во СПбГЭТУ «ЛЭТИ», 2018. 52 с.